Ab initio pair potentials from quantum-mechanical atoms-in-crystals calculations



1993 J. Phys.: Condens. Matter 5 4975

(http://iopscience.iop.org/0953-8984/5/28/012)

J. Phys.: Condens. Matter 5 (1993) 4975–4988. Printed in the UK

# *Ab initio* pair potentials from quantum-mechanical atoms-in-crystals calculations

J M Recio, E Francisco, M Flórez and A Martín Pendás

Departamento de Química Física y Analítica, Facultad de Química, Universidad de Oviedo, 33006 Oviedo, Spain

Received 7 October 1992, in final form 26 February 1993

**Abstract.** A new technique for deriving pairwise potentials from *ab initio* quantum-mechanical calculations of atoms in crystals is presented. The total energy of the crystal referred to the infinitely separated atoms is partitioned into two components: (i) a monocentric *deformation* energy arising from the changes of atomic electron density in passing from the free atom to the crystal state, and (ii) a bicentric energy due to the atomic interactions in the crystal. We show that the first component can be meaningfully separated into pairwise contributions. The new technique is used to derive Buckingham-type potentials for the alkali chloride crystals that (a) reproduce the *ab initio* crystal energy, (b) predict good static equations of state and defect properties, and (c) give a realistic description of the crystal binding.

## 1. Introduction

An increasing interest in deriving reliable pairwise interatomic potentials (IPs) from *ab initio* potential energy surfaces (PESs) has evolved in the last few years [1–8]. This approach has the advantage of making possible the theoretical study of systems such as dilute impurity crystals [1–4], or experimentally unknown polymorphs [6–8], for which the methods of deriving empirical IPs are difficult to apply. *Ab initio* PESs are also a major quality test for the theoretical strategies adopted in pair-potential work, as Lu and Hardy [7] have recently discussed for Gordon–Kim IPs [9] in $K_2SeO_4$.

The IPs can be generated by fitting analytical expressions for the interatomic interactions to a discrete collection of points of the *ab initio* PES. This procedure is useful when dealing with a single pair of atomic species. Recent examples are the first-neighbours IPs for impurity-doped alkali halides derived by Pandey *et al* [1–4], or the metal–metal IP obtained by Blaisten-Barojas and Khanna [5] for beryllium clusters. However, when the PESs contain interactions between several atomic pairs, the fitting becomes ambiguous due to the many-body terms of the quantum-mechanical energy. This ambiguity means that very different IPs can give similar descriptions of the PES, as shown by van Beest *et al* [8] in their force-field calculations on silicas. This drawback may be overcome if the quantum-mechanical method gives explicitly the specific interactions we want to model, and they are used, instead of the total energy, to derive the IPs. Although this procedure takes into account the interatomic energies in a more realistic way, some arbitrariness still remains because the IPs are forced to include the many-body contributions to the PES, as computed in the *ab initio* work.

It is well known that atomic electronic densities are generally required to compute the IPs. This requirement is a source of further difficulties. For instance, in covalent systems this calls for some kind of population analysis if the LCAO approximation is used to compute

0953-8984/93/284975+14$07.50  

the PES [6, 7]. Such analysis introduces a certain amount of arbitrariness. In ionic crystals, it is frequently assumed that the system is made up of well separated ionic species with electronic densities given by the free-atom values [9]. Unfortunately, it has been shown that considerable changes in the electronic densities appear in passing from the gas phase to the crystal, especially for negative ions [10–13].

Consideration of all these difficulties lead us to use, as the starting point in deriving *ab initio* IPs, an atom-in-the-crystal scheme able to give crystal-consistent electronic densities, accurate deformation energies, and detailed interatomic interactions. The *ab initio* perturbed ion (*ai*PI) method recently developed in our laboratory [10–13] has been our choice. This is a Hartree–Fock (HF) method based on the theory of electronic separability (TES) [14–16] and capable of including monocentric correlation energy corrections. It has been successfully applied to a great variety of crystals and properties.

In this work we derive reliable pair potentials from *ai*PI PESs of ACl (A: Li, Na, K, Rb) crystals. Thus, atomic and interaction *ai*PI energies for every different atom in the crystal are computed over a wide range of geometrical parameters. Then, the many-body part of the cohesive energy is partitioned into pairwise contributions by means of a new scheme introduced here.

We paid particular attention to the following five factors: (a) recovering the original PES and equilibrium properties by the proposed IPs, (b) relative importance of the different interaction terms to the crystal binding, (c) intercrystal transferability of the Cl–Cl pair potentials, (d) comparison of our *ab initio* IPs with several state-of-the-art empirical IPs [17], and (e) applicability of the IPs to obtain defect properties.

Our results show that the IPs generated in this work are fully consistent with the quantum-mechanical description of the whole system. In this sense, our work is similar to the method proposed by Pandey *et al* [1–4] to derive IPs from ICECAP calculations, but differs from the work by Lu and Hardy [7] on $K_2SeO_4$, and by Tsuneyuki *et al* [6] and van Beest *et al* [8] on silica, who prepare IPs from quantum-mechanical calculations on small subsets of the crystal.

In the next section we present our generating scheme. Section 3 contains the results and the discussion. Concluding remarks and future prospects are given in the last section.

## 2. Method

The description of the *ai*PI method is given in references [10]–[13]. According to this model, the lattice energy $E_{\text{latt}}$ of the crystal is given by (see equations (19) and (20) of [10])

$$E_{\text{latt}} = E_{\text{cryst}} - \sum_{A=1}^{N} E_0^A = \sum_{A=1}^{N} \left( E_{\text{def}}^A + \tfrac{1}{2} \sum_{S \neq A}^{N} E_{\text{int}}^{AS} \right) \tag{1}$$

where $E_{\text{cryst}}$ is the total energy of the crystal, $E_0^A$ is the gas-phase energy of atom $A$, and $A$ sums over the atoms in the crystal.

$E_{\text{def}}^A$ is the self-energy of the atom $A$ upon crystal formation and $E_{\text{int}}^{AS}$ is the interaction energy between atoms $A$ and $S$. $E_{\text{def}}^A$ is given by

$$E_{\text{def}}^A = E_{\text{net}}^A - E_0^A = \langle \Psi_A | H_0^A | \Psi_A \rangle - E_0^A \tag{2}$$

where $\langle \Psi_A | H_0^A | \Psi_A \rangle$ is the expectation value of the free-atom Hamiltonian over the crystal-optimized wave function of atom $A$. Since $\Psi_A$ is crystal consistent [10], $E_{\text{def}}^A$ incorporates many-body contributions into the lattice energy.

In pair-potential theory $E_{\text{latt}}$ is supposed to be expressible as

$$E_{\text{latt}} = \tfrac{1}{2}\sum_{A=1}^{N}\sum_{S\neq A}^{N} E_{\text{pair}}^{AS} \tag{3a}$$

with the symmetry condition

$$E_{\text{pair}}^{AS} = E_{\text{pair}}^{SA}. \tag{3b}$$

We have now to connect the magnitudes in equation (1) with those in equation (3*a*). In order to do so, we write the many centre deformation energy in the form

$$E_{\text{def}}^{A} = \sum_{S\neq A} E_{\text{def}}^{AS} + \sum_{S,T\neq A} E_{\text{def}}^{AST} + \ldots. \tag{4}$$

Equations (1) and (3*a*) can be identified if all terms but the first one are neglected in equation (4), i.e., if the deformation energy can be partitioned into two-centre contributions. Absorbing the small high-order contributions into the pairwise term, the IPs derived will thus include many-body interactions implicitly.

Using equation (4), we can write the lattice energy in equation (1) as

$$E_{\text{latt}} = \sum_{A=1}^{N}\sum_{S\neq A}^{N}(E_{\text{def}}^{AS} + \tfrac{1}{2}E_{\text{int}}^{AS}). \tag{5}$$

Equations (3*a*) and (5) have the same number of terms but equation (5) does not necessarily fulfill the symmetry requirement of equation (3*b*). To satisfy this, we define an average deformation energy for atoms $A$ and $S$,

$$\langle E_{\text{def}}^{AS}\rangle = \tfrac{1}{2}(E_{\text{def}}^{SA} + E_{\text{def}}^{AS}). \tag{6}$$

that gives

$$E_{\text{latt}} = \sum_{A=1}^{N}\sum_{S\neq A}^{N}(\langle E_{\text{def}}^{AS}\rangle + \tfrac{1}{2}E_{\text{int}}^{AS}). \tag{7}$$

This form can be directly compared with equation (3*a*), leading to the *key equation*

$$E_{\text{pair}}^{AS} = 2\langle E_{\text{def}}^{AS}\rangle + E_{\text{int}}^{AS}. \tag{8}$$

Equation (8) provides a non-empirical procedure to compute the pairwise interatomic energy between two atoms. We note the following: (a) $E_{\text{int}}^{AS}$ should be computed using environment-consistent descriptions for all atoms in the crystal, (b) a reasonable algorithm to compute $\langle E_{\text{def}}^{AS}\rangle$ is needed, and (c) the interaction energy between a pair of species will change from crystal to crystal due to changes in deformation and interaction terms. This prevents an exact transferability of the IPs among different crystals or even different phases of a given compound.

To obtain $\langle E_{\text{def}}^{AS}\rangle$ from *ai*PI calculations we used the following scheme. First, we classify the environment of the atom $A$ into shells of neighbours. The shells are ordered by increasing

distance from $A$. All the ions in a shell are identical and crystallographically equivalent. The contribution to $E^A_{\rm def}$ assigned to an ion of the $k$th shell is computed as

$$E^{Ak}_{\rm def} = (1/n_k)(\langle\Psi_A^{12\ldots k}|H_0^A|\Psi_A^{12\ldots k}\rangle - \langle\Psi_A^{12\ldots(k-1)}|H_0^A|\Psi_A^{12\ldots(k-1)}\rangle) \tag{9}$$

where $n_k$ is the number of ions in the $k$th shell, and $\Psi_A^{12\ldots k}$ the wave function computed through an *ai*PI calculation in which the environment is formed only by the first $k$ shells. For the ions in the first shell we define

$$E^{A1}_{\rm def} = (1/n_1)(\langle\Psi_A^1|H_0^A|\Psi_A^1\rangle - E_0^A). \tag{10}$$

The function $\Psi_A^{12\ldots k}$ changes upon compressing or expanding the lattice. Thus, these pairwise deformation energies depend on the crystal geometry.

The whole process of deriving the pair potentials for a given crystal and geometry consists, then, of a collection of different *ai*PI calculations. Starting with the free-ion description, the wave functions for the ions in the crystal are successively refined by introducing the shells of neighbours one at a time. Finally, an *ai*PI run is performed for the complete crystal in which every ion is self-consistently modified by all its neighbours. The interaction energies are computed from the group functions obtained at this last step.

## 3. Pairwise potentials for alkali chloride crystals

To examine the strengths and limitations of our method, we prepared IPs for the rock-salt phase of four alkali chloride crystals (ACl, A: Li, Na, K, and Rb). The *ai*PI crystal energy and the interaction and deformation pair energies have been computed for a wide range of values of the lattice parameter $a$. The Coulomb–Hartree–Fock electron correlation correction of Chakravorty and Clementi [18] has been included in the calculation.

**Table 1.** Buckingham-type pair potentials computed in this work for the alkali chlorides. Atomic units are used throughout. The symbols + and − stand for cation and anion, respectively.

| Crystal | Ion pair | $A$ | $\alpha$ | $B$ | $n$ |
|---|---|---|---|---|---|
| LiCl | ++ | — | — | — | — |
| | +− | 110.801 955 | 2.153 669 30 | — | — |
| | −− | 7.604 680 10 | 0.960 827 682 | 696.029 494 | 6 |
| NaCl | ++ | — | — | — | — |
| | +− | 356.517 087 | 2.160 743 25 | — | — |
| | −− | 2.668 295 14 | 0.866 344 682 | 551.810 140 | 6 |
| KCl | ++ | 6077.067 18 | 2.627 425 68 | 0.116 709 28 | 6 |
| | +− | 53.901 590 4 | 1.506 705 89 | — | — |
| | −− | — | — | 8912.915 50 | 8 |
| RbCl | ++ | — | — | 159 850.057 | 10 |
| | +− | 33.715 601 3 | 1.366 219 55 | — | — |
| | −− | — | — | 13 103.303 8 | 8 |

*To obtain the function $E^{AS}_{\rm pair}(R)$, we determine the deformation and interaction energies* appearing in the *key equation*, equation (8), for a collection of distances, $R$, between centres $A$ and $S$. We can imagine two different ways of doing this. First, at a single crystal geometry, a given species will appear in different shells of neighbours, each characterized

by a particular distance from the central ion. Second, we can use data from a single shell and perform calculations for different crystal geometries. These two approaches give slightly different results, partly because the partition of the deformation energy is arbitrary. Since the fitting procedure for the potentials derived for the nearest neighbours will be more accurate, we follow the second approach here.

The interionic energies have been represented by an analytical expression formed by a point-charge term involving the nominal charge of each ion, plus a short-range Buckingham term:

$$V = A\exp(-\alpha R) - B/R^n. \tag{11}$$

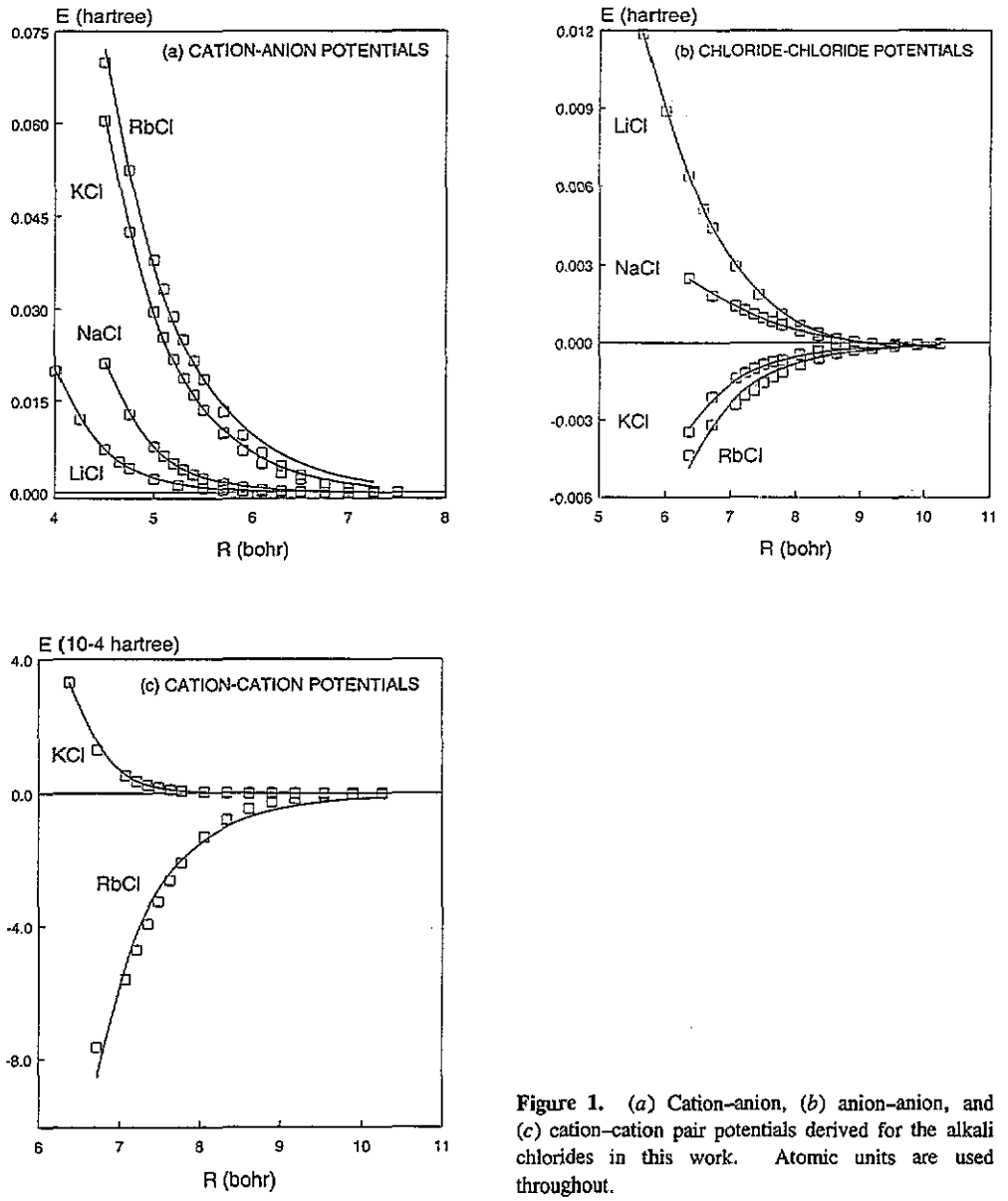


**Figure 1.** (*a*) Cation–anion, (*b*) anion–anion, and (*c*) cation–cation pair potentials derived for the alkali chlorides in this work. Atomic units are used throughout.

Values of $A$, $\alpha$, $B$, and $n$ for cation–cation (++), cation–anion (+−), and anion–anion (−−) pairs in LiCl, NaCl, KCl, and RbCl are collected in table 1. The ++ interactions in LiCl and NaCl are very small and have been neglected. The pair potentials obtained from the *ai*PI PES will be called here PIIPs.

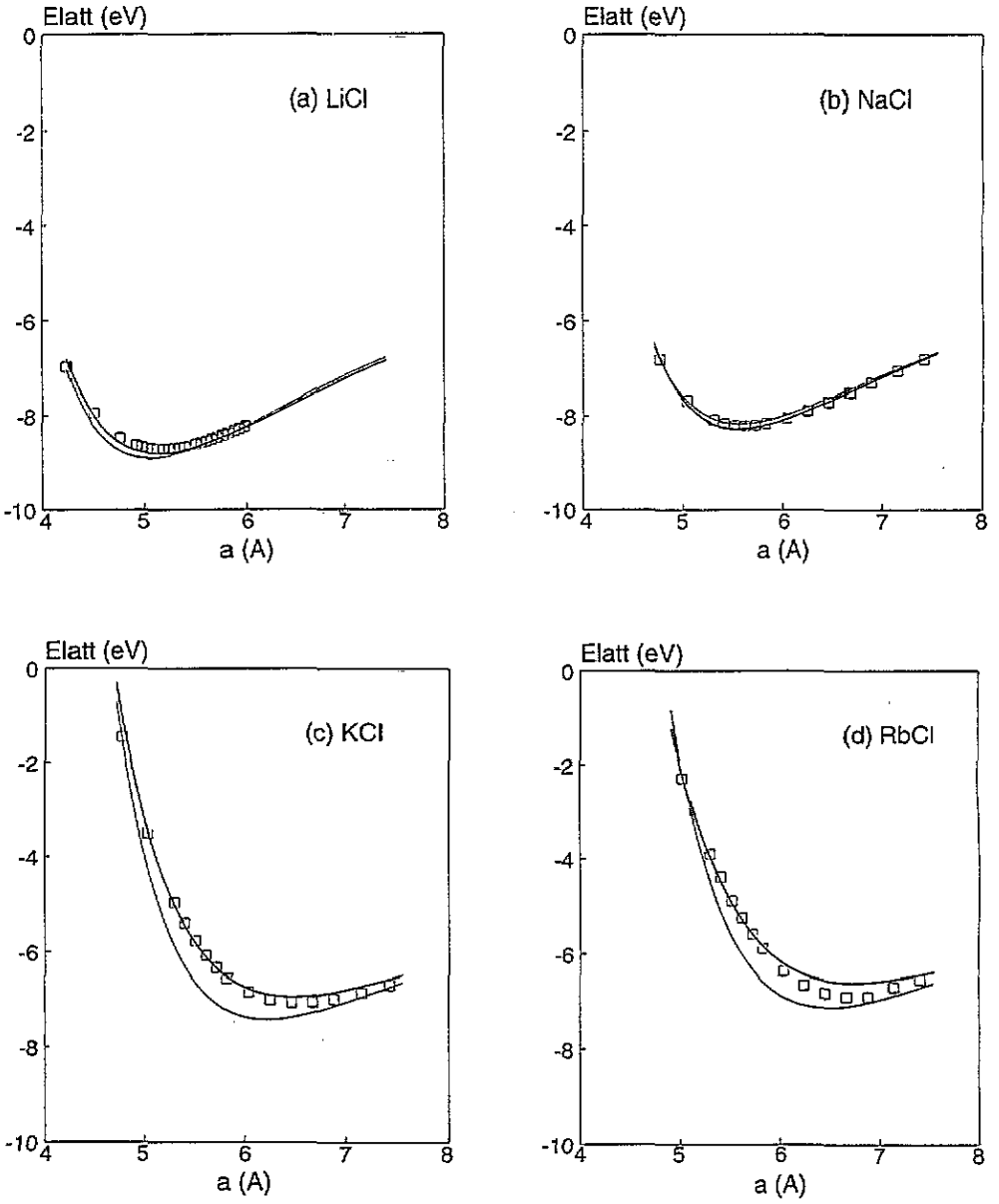


**Figure 2.** Lattice energy of (*a*) LiCl, (*b*) NaCl, (*c*) KCl, and (*d*) RbCl. Bold and fine curves correspond to the theoretical interaction potentials of this work and the empirical interaction potentials of Catlow *et al* [17], respectively. Squares are the *ai*PI results.

The $R$ dependence of the Buckingham part is plotted in figure 1. All +− short-range interactions are repulsive and can be well represented by an exponential term. Their

magnitude increases from Li–Cl to Rb–Cl. Li–Cl and Na–Cl pairs behave in a similar way, as do the K–Cl and Rb–Cl pairs. The Cl–Cl interactions are much smaller. They are repulsive for LiCl and NaCl but attractive for KCl and RbCl. The cation–cation interactions are even smaller.

These properties of the potentials are related to the predicted geometries. Most remarkably, the conspicuous differences among the Cl–Cl potentials suggest difficulties in the transferability of the potentials.

### *3.1. Equilibrium properties and the PES test*

To examine the quality of the PIIPs, we compute with them the lattice energy of their respective ACl crystals. All interactions larger than one nanohartree have been included. The calculations were repeated with the empirical IPs of Catlow *et al* [17] (set I), called here EMIPs. In figure 2 we show the results as well as the *ai*PI curves. The PIIP curves reproduce very well the *ai*PI values, showing that the arbitrariness in the generation of the potentials does not introduce unacceptable errors. Some discrepancies between the PIIP and EMIP curves appear in the four crystals, especially in KCl and RbCl.

The equilibrium lattice parameter $a_e$ and the lattice energy $E_{latt}$ derived from the PIIP, EMIP, and *ai*PI calculations are collected in table 2. For comparison, we have included predictions from the local density approximation [19, 20] and self-consistent tight-binding calculations [21]. The observed values or the low-temperature extrapolations are also shown. The best prediction of $a_e$ is given by the EMIPs because they were calibrated using this quantity. Interestingly enough, differences between EMIP and PIIP calculations are smaller than 0.30 Å for $a_e$ and 0.44 eV for $E_{latt}$. Note that our set of computed equilibrium values compares with the experimental data as well as the corresponding predictions from other solid-state calculations. Also, the PIIPs reproduce the equilibrium properties computed with the *ai*PI method well.

**Table 2.** Equilibrium lattice parameter $a_e$ (Å) and lattice energy $E_{latt}$ (eV) for the alkali halides, according to several sources: PIIPs: theoretical pair potentials of this work; EMIPs: empirical pair potentials of Catlow *et al* [17]; *ai*PI: *ab initio* perturbed ion calculations [24]; other solid-state calculations, and low-temperature experimental data.

| | | Crystal | | | |
|---|---|---|---|---|---|
| | | LiCl | NaCl | KCl | RbCl |
| $a_e$ | PIIPs | 5.128 | 5.540 | 6.464 | 6.746 |
| | EMIPs | 5.048 | 5.556 | 6.211 | 6.477 |
| | *ai*PI | 5.182 | 5.600 | 6.534 | 6.782 |
| | Other calculations | 5.32 [19] | 5.737 [19] | 6.30 [19] | |
| | | | 5.52 [20] | 6.30 [20] | |
| | | | 5.744 [21] | 6.242 [21] | 6.400 [21] |
| | Experimental [22] | 5.078 | 5.578 | 6.232 | 6.517 |
| $-E_{latt}$ | PIIPs | 8.76 | 8.30 | 6.95 | 6.61 |
| | EMIPs | 8.90 | 8.20 | 7.38 | 7.13 |
| | *ai*PI | 8.71 | 8.22 | 7.07 | 6.92 |
| | Other calculations | | 7.94 [21] | 7.82 [21] | 7.76 [21] |
| | Experimental [23] | 8.76 | 8.02 | 7.37 | 7.03 |

### *3.2. Pair potentials and crystal binding*

The non-classical energy of a crystal can be shared out in several ways by the different types of pair. Meng *et al* [3] have pointed out that some of these distributions can fit equally well a given set of macroscopic data. However, in the present method, the distribution of this energy ($\cong$ 11% of $E_{latt}$) among the three kinds of interaction (++, +−, and −−) is uniquely determined. Although there is no experimental procedure to identify the relative role of the ++, +−, and −− interactions, we think that some theoretical requirements should be imposed upon the IPs. One of these tests is the consistency of similar interactions for a family of compounds.

We collect in table 3 the ++, +−, and −− contributions to $E_{latt}$ computed with the PIIPs and the EMIPs. The ++ interactions play a minor role due to small cation polarizability and large intercationic separations in the ACl crystals. In the PI and EM pictures these interactions behave quite alike, although a greater stabilization is given by the EMIPs when the cation size increases.

**Table 3.** Distribution of the non-classical energy among the three kinds of pair in alkali halides. First row: theoretical pair potentials calculated in this work. Second row: empirical pair potentials from Catlow *et al* [17]. Units are eV for energies and Å for distances.

| Crystal | ++ | +− | −− | $-E_{latt}$ | $-E_{latt}$ | $a_e^a$ | $a_e$ |
|---|---|---|---|---|---|---|---|
| LiCl | 0.00 | 0.53 | 0.62 | 8.66 | 8.80 | 5.164 | 5.128 |
| | −0.00 | 0.96 | 0.11 | 8.90 | 8.90 | 5.046 | 5.048 |
| NaCl | 0.00 | 0.71 | 0.17 | 8.20 | 8.27 | 5.560 | 5.541 |
| | −0.05 | 0.97 | −0.01 | 8.14 | 8.16 | 5.564 | 5.557 |
| KCl | 0.00 | 0.89 | −0.05 | 6.94 | 6.94 | 6.464 | 6.465 |
| | −0.10 | 0.93 | −0.10 | 7.37 | 7.37 | 6.232 | 6.211 |
| RbCl | −0.01 | 0.91 | −0.05 | 6.61 | 6.61 | 6.745 | 6.746 |
| | −0.11 | 0.95 | −0.13 | 7.07 | 7.12 | 6.506 | 6.477 |

[a] Including only the nearest interactions between each pair.

The +− interactions contribute differently to the two sets of potentials. Within the EMIP picture, this contribution is very similar in the four ACl crystals but the PIIP values increase clearly with the cation size. We think that the latter picture is more realistic. In passing from the two-electron $Li^+$ to the 36-electron $Rb^+$, we expect the short-range +− interaction to increase, no matter how large the interionic separation may be. This is what the PIIPs predict.

The −− contribution is also different for the two sets. The $Cl^-$ ion reduces its volume from LiCl to RbCl due to the increasing size and decreasing polarization ability of the cation. Thus, we expect a decreasing −− contribution to the lattice energy in this direction. This is the behaviour found for the two sets, although the EMIP values are smaller. This may be due to the use of a single analytical IP for the four crystals.

The last four columns of table 3 show the predictions of $a_e$ and $E_{latt}$ when only the first neighbours of each type of ion are taken into account. There is an interesting conclusion from the comparison of both calculations: the equilibrium properties of the ACl crystals are almost entirely determined by the interaction between nearest and next-nearest neighbours.

### *3.3. Transferability of the chloride–chloride potential*

There is much evidence to indicate that the chloride ion has different electronic density in different ACl crystals. This raises doubts about the IP transferability. For instance, Meng

*et al* [3] examined the $Ag^+$–$Cl^-$ IP in $Ag^+$:NaCl, $Ag^+$:KCl, and $Ag^+$:RbCl by computing the activation energy for $Ag^+$ diffusion. They concluded that the IP transferability in these cases is not good. In line with this, we have already shown that the Cl–Cl interaction changes considerably from crystal to crystal. It could be argued, however, that when the +− short-range terms are the dominant interaction, the equilibrium crystal properties could be well reproduced even if the Cl–Cl IPs for each system differ. To test this assumption, we computed the equilibrium properties of each crystal with the Cl–Cl PIIPs derived from all other crystals (table 4).

**Table 4.** Equilibrium lattice parameter $a_e$ (Å) and lattice energy $E_{latt}$ (eV) for the alkali chlorides computed with Cl–Cl potentials derived for LiCl, NaCl, KCl and RbCl.

| | $a_e$ Cl–Cl potential derived for | | | | $E_{latt}$ Cl–Cl potential derived for | | | |
|---|---|---|---|---|---|---|---|---|
| Crystal | LiCl | NaCl | KCl | RbCl | LiCl | NaCl | KCl | RbCl |
| LiCl | 5.128 | 4.868 | 4.446 | 4.178 | 8.80 | 9.18 | 10.18 | 10.78 |
| NaCl | 5.647 | 5.540 | 5.361 | 5.313 | 8.17 | 8.28 | 8.58 | 8.70 |
| KCl | 6.575 | 6.547 | 6.465 | 6.442 | 6.92 | 6.91 | 6.95 | 6.97 |
| RbCl | 6.843 | 6.827 | 6.764 | 6.746 | 6.60 | 6.58 | 6.59 | 6.61 |

Results for LiCl and, to a lesser extent, NaCl are highly dependent on the Cl–Cl potential used. Dispersions as large as 1.2 Å in $a_e$ and 2.0 eV in $E_{latt}$ are found in LiCl. The situation is not so bad in the other crystals. For RbCl, $a_e$ and $E_{latt}$ are relatively independent of the origin of the Cl–Cl potentials. $E_{latt}$ is, in any case, less sensitive than $a_e$. As expected from the curves in figure 1, the IPs derived from KCl and RbCl produce comparable results. The different behaviour observed in the four crystals is a measure of the relative importance of the −− interactions with respect to the dominant +− terms.

As a general conclusion, we believe that there is not a single Cl–Cl potential adequate for the four alkali chlorides. The Cl–Cl IP may be enforced to give accurate predictions of equilibrium properties for the ACl crystals only because in KCl and RbCl this interaction plays a secondary role. Our analysis suggests that the physical relevance of this enforced parametrization is uncertain.

### *3.4. Static equations of state at 0 K*

The static equation of state (EOS) at 0 K can be computed from $E_{latt}(a)$ by means of the relation

$$P = -(\partial E_{latt}/\partial a)(\partial a/\partial V) \tag{12}$$

where $P$ is the hydrostatic pressure and $V$ the molar volume, $V = \frac{1}{4}a^3$.

A number of detailed $P$–$V$ diagrams have been prepared [24] using equation (12) and our PIIPs. We compare here these EOSs with an empirical EOS very useful for real solids. The fact that the PIIPs have been developed performing calculations at different crystal geometries provides our interatomic potentials with a special ability to simulate the $P$–$V$ behaviour. We have chosen the *universal* EOS of Vinet *et al* [25] as a measure of the quality of our crystal simulation. This EOS has recently been tested for a wide variety of compounds, including alkali chlorides. Its overall performance makes this equation an appropriate benchmark in

EOS work [26,27]. The EOS of Vinet *et al* [25] connects isothermal $P$–$V$ data through the relation

$$\ln H = \ln B_0 + \tfrac{3}{2}(B_0' - 1)(1 - x) \tag{13}$$

where $H$ and $x$ are defined as

$$H = Px^2/(3(1-x)) \qquad x = (V/V_0)^{1/3} \tag{14}$$

where $V_0$, $B_0$ and $B_0'$ are the volume, the isothermal bulk modulus, and its first pressure derivative, respectively, at zero pressure.

We show in figure 3 the results of this test. The squares are theoretical points calculated with the PIIPs. Straight lines are the best fitted Vinet EOSs. We see a very good agreement between the behaviour predicted by the PIIPs and that given by the *universal* equation. The crystals simulated by the PIIPs obey the Vinet EOS with linear correlation coefficients larger than 0.9998.

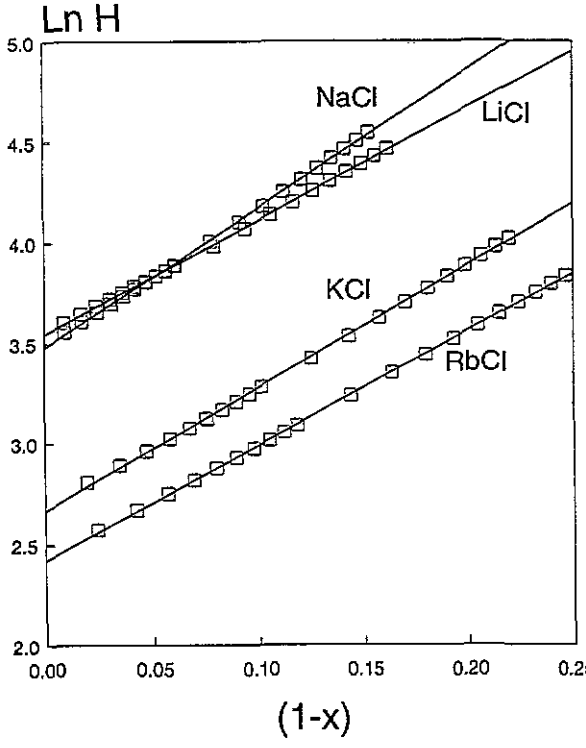


**Figure 3.** EOSs derived from our pair potentials for the four crystals (squares). Full lines are the fit to the Vinet *et al universal* equations (13) and (14).

Zero-temperature experimental data for $B_0$ and $B_0'$ are not accessible. Their finite-temperature behaviour depends upon vibrational effects neglected in this work. $B_0$ increases and $B_0'$ decreases as $T$ goes to 0. Our PIIP computed values for $B_0$ are (in GPa) 32 (LiCl), 25 (NaCl), 18 (KCl) and 16 (RbCl), which compare reasonably well with the experimental series quoted by Cohen and Gordon [28]: 35.4 (LiCl), 28.5 (NaCl), 20.2 (KCl) and 18.5 (RbCl). Thus, our predictions follow the trend shown by experimental data: $B_0$ decreases from LiCl to RbCl. The range obtained with the PIIPs for $B_0'$ ($5.1 \pm 0.4$) also lies within the expected interval at low temperature [29].

In view of these results, we may conclude that the present atomistic simulation of the ACl crystals is adequate since the theoretical EOS is consistent with those empirically deduced from real solids, and the predictions of the elastic properties are good.

### *3.5. Substitutional alkali impurities in alkali chloride crystals*

As another example of the applicability of our PIIPs, we report some defect calculations of impurities in alkali chloride crystals using the HADES program [30]. The short-range nature of the deformation energy, and its fast convergence with the interatomic separation, provide a reasonable justification of our present pairwise division in defect calculations. It is important to keep in mind that the deformation energy contribution to the PIIPs takes into account the local environment surrounding each atom. This is particularly convenient when dealing with defect properties.

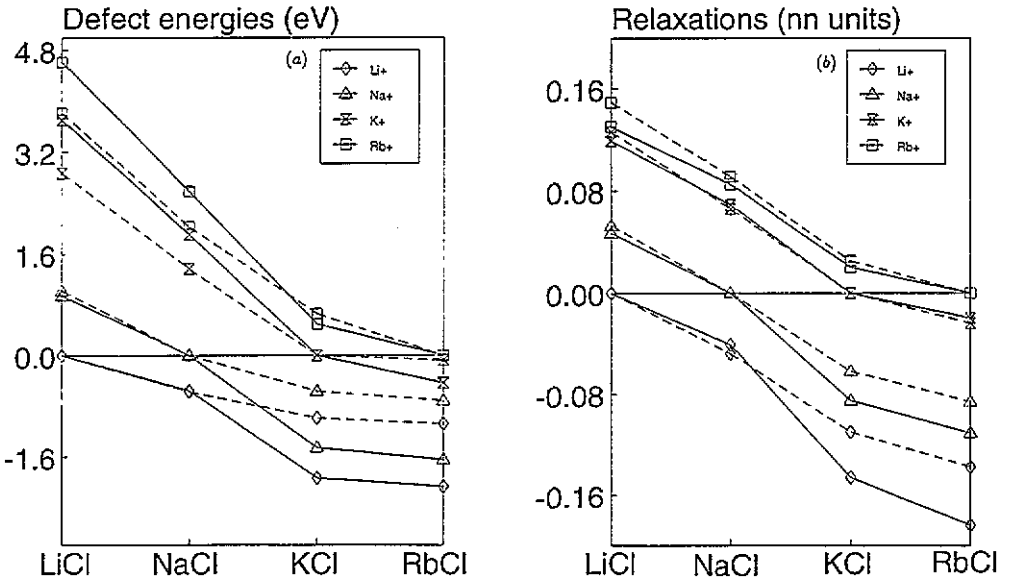


**Figure 4.** (*a*) Defect energies and (*b*) local relaxations (in nearest-neighbour (NN) units) of alkali cations in alkali chloride crystals. Full and broken lines refer to PIIPs and EMIPs, respectively.

We study the defect energies of alkali impurities ($Li^+$, $Na^+$, $K^+$, and $Rb^+$) at the substitutional sites of the host crystals. In these calculations we allow 122 ions around the impurity to move to their minimum-energy configuration, keeping the rest of ions in their crystallographic positions. The geometrical distortions are important for the impurity nearest neighbours and decrease for the most distant host ions to values less than 0.1% of the lattice parameter. Therefore, the interface between the two regions becomes very smooth. The interesting feature to emerge from these calculations is that defect energies and nearest-neighbour relaxations are mainly determined by the differences between the impurity–chloride and host-cation–chloride short-range potentials. The substitutional impurity breaks the equilibrium stage of the perfect lattice because its short-range interaction energy with the chloride ions does not match that of the cation host. If the impurity–chloride interaction is smaller than the cation host–chloride one, the chloride ions move towards the impurity to restore the zero-force conditions at the ions. In consequence, we expect to have impurity–chloride distances less than $\frac{1}{2}a_e$ and negative defect energies in this case. On the other hand, when the impurity–chloride short-range interaction is larger than the cation host–chloride one, an outward relaxation of the nearest neighbours around the impurity minimizes the extra repulsive energy introduced by the defect in the lattice.

Our results in figure 4 (full lines) are consistent with the above argument. The curves show the expected regularities according to the cation–anion potentials plotted in figure 1(*a*). Given a host lattice, values of defect energies and nearest-neighbour relaxations can be sorted in the order $Li^+ < Na^+ < K^+ < Rb^+$. Furthermore, defect energies of impurities and local relaxations decrease from LiCl to RbCl. Outward/inward relaxations around the impurity always occur along with positive/negative defect energies. It is important to notice here that the trend in the impurity–chloride distances is fully consistent with the arguments based on the ion sizes.

We compare again our results with those obtained using the EMIP set (broken lines in figure 4). Overall, the empirically derived potentials also provide the above-mentioned trends, although the defect energy is only −0.07 eV for the $K^+$ ion in RbCl. For the relaxations, the discrepancies in the predicted values are less than 5%. With respect to the calculated EMIP defect energies, a smaller variation is observed in passing from LiCl to RbCl, in accordance with the differences between the cation–anion interaction energies in these sets (see table 3).

We have also explored the off-centre displacements of substitutional $Li^+$ in NaCl, KCl, and RbCl. There is a well documented knowledge of the off-centre position along the ⟨111⟩ direction of $Li^+$ in KCl [31,32]. [31] also gives experimental evidence of on-centre locations for $Li^+$ in NaCl and RbCl. However, the more recent [32] gives experimental results showing an off-centre position for $Li^+$ in RbCl. As quoted in this article, calculations of off-centre behaviour are a delicate test both of the simulation technique and of the potentials employed. Using the PIPs we have obtained the potential-energy curves of $Li^+$ in the three host crystals along the ⟨111⟩ direction, as plotted in figure 5. Our results predict an on-centre position of $Li^+$ in NaCl, but an increasing preference for off-centre positions in KCl and RbCl.

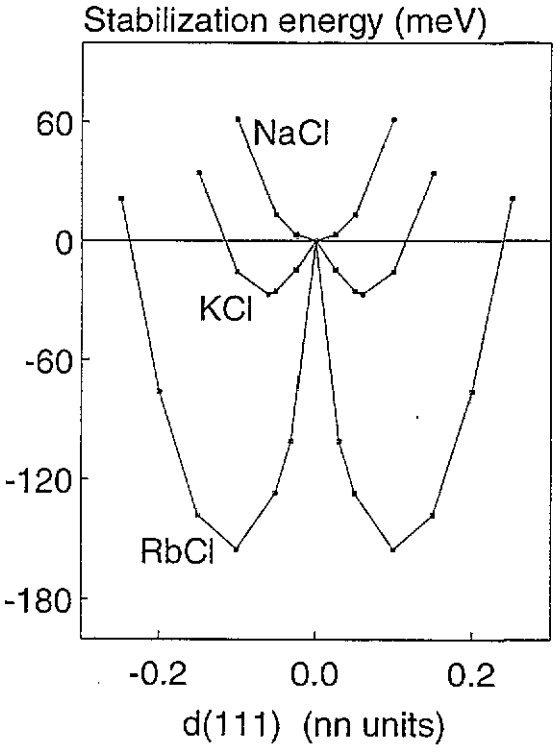


**Figure 5.** Stabilization energy from the $d(111)$ displacement (in nearest-neighbour (NN) units) in $Li^+$:ACl (A=Na, K, Rb).

This behaviour also agrees with that obtained from other well established methods. In particular, our values for the $Li^+$ ⟨111⟩ equilibrium displacements in NaCl, KCl and RbCl lattices (0, 0.065 and 0.110 in units of the anion–cation nearest-neighbour (NN) distance, respectively) agree very well with those obtained by Fitzsimons *et al* [33] (0, 0.069 and 0.134, respectively), whereas values of Catlow *et al* [34] with the EMIPs are somewhat higher (0, 0.117 and 0.156, respectively).

## 4. Conclusions and prospects

A method to obtain IPs from *ab initio* quantum-mechanical calculations has been developed and tested in four alkali chloride crystals. The method is considerably demanding because the IPs are constrained to recover (a) the original energy surfaces and (b) the individual energetic components for each different pair of atoms in the system. The potentials derived for the chlorides have been successfully examined by means of several theoretical and empirical tests. These potentials provide a realistic description of the equilibrium properties, static EOSs and defect properties of alkali chlorides. Besides this satisfactory macroscopic description, the PIIPs collect in a reliable way the physical behaviour of the three different interionic interactions operating in the crystals.

Improvements in the method are in progress in our laboratory. We are presently considering the following aspects: (a) introduction of dynamical correlation effects into the reference *ai*PI formalism; (b) inclusion of explicit three-body interactions in the IPs by means of a more complex partition of the deformation energy, and (c) use of multi-variable functions to fit the *ab initio* interionic energies.

## Acknowledgments

Thanks are due to the Vicerrectorado de Investigación, Universidad de Oviedo, for the CONVEX-VAX facility and grant DF91/22146. Financial support from the Dirección General de Investigación Científica y Técnica (DGICyT), project PB90-0795, is gratefully acknowledged. We want to thank Professor L Pueyo and V Luaña for many encouraging discussions and the careful reading of the manuscript. JMR thanks the Spanish Ministerio de Educación y Ciencia for the concession of a Fulbright grant that made possible his stay at the Michigan Technological University. JMR is also very grateful to Professor R Pandey for many stimulating discussions and the opportunity to use the HADES program.

## References

[1] Meng J, Pandey R, Vail J M and Kunz A B 1988 *Phys. Rev.* B **38** 10083
[2] Pandey R and Vail J M 1989 *J. Phys.: Condens. Matter* **1** 2801
[3] Meng J, Pandey R, Vail J M and Kunz A B 1989 *J. Phys.: Condens. Matter* **1** 6049
[4] Pandey R, Zuo J and Kunz A B 1990 *J. Mater. Res.* **5** 623
[5] Blaisten-Barojas E and Khanna S N 1988 *Phys. Rev. Lett.* **61** 1477
[6] Tsuneyuki S, Tsukada M, Aoki H and Matsui Y 1988 *Phys. Rev. Lett.* **61** 869
[7] Lu H M and Hardy J R 1990 *Phys. Rev. Lett.* **64** 661
[8] van Beest B W H, Kramer G J and van Santen R A 1990 *Phys. Rev. Lett.* **64** 1955
[9] Gordon R and Kim Y S 1972 *J. Chem. Phys.* **56** 3122
[10] Luaña V and Pueyo L 1990 *Phys. Rev.* B **41** 3800
[11] Luaña V, Recio J M and Pueyo L 1990 *Phys. Rev.* B **42** 1791

[12] Luaña V, Flórez M, Francisco E, Martín Pendás A, Recio J M, Bermejo M and Pueyo L 1992 *Cluster Models for Surface and Bulk Phenomenon (NATO ASI Ser. B: Physics)* vol 283, ed G Pacchioni, P S Bagus and F Parmigiani (New York: Plenum) p 605
[13] Pueyo L, Luaña V, Flórez M and Francisco E 1992 *Structure, Interactions and Reactivity* vol B, ed S Fraga (Amsterdam: Elsevier) p 504
[14] McWeeny R 1959 *Proc. R. Soc.* A **253** 242; 1989 *Methods of Molecular Quantum Mechanics* (London: Academic)
[15] Huzinaga S and Cantu A A 1971 *J. Chem. Phys.* **55** 5543
[16] Huzinga S, McWilliams D and Cantu A A 1973 *Adv. Quantum Chem.* **7** 187
[17] Catlow C R A, Diller K M and Norgett M J 1977 *J. Phys. C: Solid State Phys.* **10** 1395
[18] Chakravorty S J and Clementi E 1989 *Phys. Rev.* A **39** 2290
[19] Yamashita J and Asano S 1983 *J. Phys. Soc. Japan* **52** 3506
[20] Froyen S and Cohen M L 1984 *Phys. Rev.* B **29** 3770; 1986 *J. Phys. C: Solid State Phys.* **19** 2623
[21] Straub G K and Harrison W A 1989 *Phys. Rev.* B **39** 10325
[22] Ghate P B 1965 *Phys. Rev.* **139** 1666
[23] Kittel C 1971 *Introduction to Solid State Physics* 4th edn (New York: Wiley)
[24] Recio J M, Martín Pendás A, Francisco E, Flórez M and Luaña V to be published
[25] Vinet P V, Ferrante J, Smith J R and Rose J H 1986 *J. Phys. C: Solid State Phys.* **19** L467
[26] Sikka S K 1989 *Phys. Lett.* **135A** 129
[27] Li-Rong C and Qing-Hu C 1991 *J. Phys.: Condens. Matter* **3** 775
[28] Cohen J and Gordon R G 1975 *Phys. Rev.* B **12** 3228
[29] Birch F 1986 *J. Geophys. Res.* **91** 4949
[30] Norgett M J *UKAEA Report* AERE-R.7650
[31] Bridges F 1975 *Crit. Rev. Solid State Sci.* **5** 1
[32] Jacobs P W M 1989 *J. Chem. Soc. Faraday Trans. II* **85** 415
[33] Fitzsimons P B, Corish J and Jacobs P W M 1987 *Cryst. Latt. Def. Amorph. Mater.* **15** 7
[34] Catlow R A, Diller K M, Norgett M J, Corish J, Parker B M C and Jacobs P W M 1978 *Phys. Rev.* B **18** 2739